

Article

Effect of Pre-Fatigue on the Monotonic Deformation Behavior of a Coplanar Double-Slip-Oriented Cu Single Crystal

Xiao-Wu Li ^{1,2,*}, Xiao-Meng Wang ¹, Ying Yan ¹, Wei-Wei Guo ¹ and Cheng-Jun Qi ¹

¹ Department of Materials Physics and Chemistry, School of Materials Science and Engineering, Northeastern University, No. 3-11, Wenhua Road, Shenyang 110819, China; wxm_1314@yahoo.com (X.-M.W.); yingyan@imp.neu.edu.cn (Y.Y.); gww_2016@sina.com (W.-W.G.); kakaqi@yahoo.com (C.-J.Q.)

² Key Laboratory for Anisotropy and Texture of Materials, Ministry of Education, Northeastern University, No. 3-11, Wenhua Road, Shenyang 110819, China

* Correspondence: xwli@mail.neu.edu.cn; Tel.: +86-24-8367-8479

Academic Editor: Filippo Berto

Received: 4 October 2016; Accepted: 17 November 2016; Published: 22 November 2016

Abstract: The $[\bar{2}33]$ coplanar double-slip-oriented Cu single crystals were pre-fatigued up to a saturation stage and then uniaxially tensioned or compressed to fracture. The results show that for the specimen pre-fatigued at a plastic strain amplitude γ_{pl} of 9.2×10^{-4} , which is located within the quasi-plateau of the cyclic stress-strain (CSS) curve, its tensile strength and elongation are coincidentally improved, showing an obvious strengthening effect by low-cycle fatigue (LCF) training. However, for the crystal specimens pre-fatigued at a γ_{pl} lower or higher than the quasi-plateau region, due to a low pre-cyclic hardening or the pre-induction of fatigue damage, no marked strengthening effect by LCF training occurs, and even a weakening effect by LCF damage takes place instead. In contrast, the effect of pre-fatigue deformation on the uniaxial compressive behavior is not so significant, since the compressive deformation is in a stress state more beneficial to the ongoing plastic deformation and it is insensitive to the damage induced by pre-cycling. Based on the observations and comparisons of deformation features and dislocation structures in the uniaxially deformed $[\bar{2}33]$ crystal specimens which have been pre-fatigued at different γ_{pl} , the micro-mechanisms for the effect of pre-fatigue on the static mechanical behavior are discussed.

Keywords: Cu single crystal; coplanar double slip; pre-fatigue deformation; plastic strain amplitude; tensile behavior; compressive behavior; dislocation structure

1. Introduction

The mechanical degradation of materials will gradually occur during the process of their service due to fatigue deformation and damage accumulation. Therefore, it is extremely significant to explore the influencing mechanisms of pre-fatigue deformation on the mechanical properties of materials. Recently, there have been some investigations on the effect of pre-fatigue on the uniaxial deformation behavior of some metallic polycrystals, e.g., 6061-T6 aluminum alloy [1,2], AISI 4140T steel [1,2], 304 austenitic stainless steel [3], and commercially pure Al [4,5]. However, the microstructural complexities in those polycrystalline materials will undoubtedly preclude a distinct elucidation of the micro-mechanism for the pre-fatigue effect on the static mechanical behavior. In this sense, single crystals of high-purity metals would actually be more suitable materials for such investigations.

Quite recently, we investigated the effect of fatigue pre-deformation at different plastic strain amplitudes, γ_{pl} , on the uniaxial tensile behavior of the [017] critical double-slip-oriented Cu single crystal, and found that a low-cycle fatigue training treatment on this crystal at an appropriate

plastic strain amplitude ($\gamma_{pl} = 7.0 \times 10^{-4}$) could effectively improve its static tensile properties; this phenomenon is called the strengthening effect by low-cycle fatigue training [6]. Actually, the dislocation structures induced by fatigue deformation are quite different, strongly depending upon the crystallographic orientation (especially for double-slip orientations) [7–9]. As differently-oriented Cu single crystals are adopted for fatigue pre-deformation treatments, the induced dislocation structures are different; in this case, it is important to know how the corresponding static mechanical properties will change. In light of this, the $[\bar{2}33]$ coplanar double-slip-oriented Cu single crystal was selected for the present study, focusing on the effect of fatigue pre-deformation at different γ_{pl} on its uniaxial tensile and compressive properties. Our previous work has demonstrated that the cyclic stress-strain (CSS) curve of the $[\bar{2}33]$ coplanar double-slip-oriented Cu single crystal shows a stress quasi-plateau over the γ_{pl} range of 3.0×10^{-4} – 2.0×10^{-3} [10], and the fatigue dislocation structures consist mainly of dislocation cells, the size of which decreases with increasing γ_{pl} [11,12]. In this way, the effect of dislocation cell structures induced by pre-fatigue on the static mechanical properties of Cu single crystals can be exclusively examined.

2. Experimental Section

Cu single crystal was grown from oxygen free high conductivity (OFHC) copper of 99.999% purity by the Bridgman method. The fatigue specimens with a gauge section of 7 mm \times 5 mm \times 16 mm and 70 mm in length were spark-machined from the as-grown crystal. All specimens are oriented towards $[\bar{2}33]$, and the Laue back-reflection technique was used to determine the orientation of the specimen. Before fatigue tests, all specimens were annealed at 800 °C for 2 h in vacuum, and then electro-polished to produce a strain-free and smooth surface. Symmetric tension-compression fatigue pre-deformation tests were performed at room temperature in air using a Shimadzu servo-hydraulic testing machine (Shimadzu, Kyoto, Japan). A triangular waveform signal with a frequency range of 0.05–0.4 Hz was used for the constant plastic strain control. The plastic resolved shear strain amplitude γ_{pl} and shear stress τ were calculated by $\gamma_{pl} = \Delta\epsilon_p/2\Omega$ and $\tau = \sigma\Omega$, where $\Delta\epsilon_p/2$ is the axial plastic strain amplitude, Ω the Schmid factor of primary slip system and σ is an average value of the peak stresses in tension and compression. The crystal specimens were firstly pre-cycled at different plastic strain amplitudes ranging from 1.3×10^{-4} to 5.3×10^{-3} up to the occurrence of saturation. The pre-fatigue testing conditions and data are listed in Table 1. After pre-fatigue tests, the fatigue specimens were spark-machined into the tensile specimens with a gauge section of 5 \times 2 \times 16 mm³ and 70 mm in length. The specimens were then polished electrolytically and subjected to tensile deformation to a final fracture at a strain rate of 10^{-3} ·s⁻¹. After tensile tests, the surface deformation characteristics of these specimens were observed by using a SSX-550 scanning electron microscope (SEM, Shimadzu, Kyoto, Japan), and the dislocation structures were observed by using a Tecnai G² 20 transmission electron microscope (TEM, FEI, Hillsboro, OR, USA) operated at 200 kV. TEM thin foils were first spark-cut from the gauge part (homogeneous deformation region near the fracture) of the fractured specimens, then mechanically thinned down to dozens of micron thick and finally polished by a conventional twin-jet method.

Table 1. Pre-fatigue testing conditions and data for the $[\bar{2}33]$ Cu single crystal [10]. Note that γ_{pl} is the plastic strain amplitude, N is the cyclic number, $\gamma_{pl,cum}$ is the cumulative plastic strain ($=4N\gamma_{pl}$), and τ_s is the saturation stress.

γ_{pl}	N	$\gamma_{pl,cum}$	τ_s , MPa
1.3×10^{-4}	65,000	33.8	25.0
3.4×10^{-4}	32,000	43.5	30.1
9.2×10^{-4}	12,000	43.5	31.7
3.5×10^{-3}	4700	65.8	33.5
5.3×10^{-3}	10,200	216.2	35.4

3. Results and Discussion

3.1. Effect of Pre-Fatigue on the Tensile and Compressive Properties

Figure 1 shows the tensile and compressive stress-strain curves of $[\bar{2}33]$ Cu single-crystal specimens unfatigued (only annealed) and pre-fatigued at different γ_{pl} , and the CSS curve of this oriented crystal [10] is also reproduced here to clearly show the location of the applied γ_{pl} in the curve. It is apparent that there is an effect of pre-cycling, to a different extent, on the tensile or compressive yield strength and the ultimate tensile strength of the crystal, depending on the γ_{pl} imposed in pre-cycling.

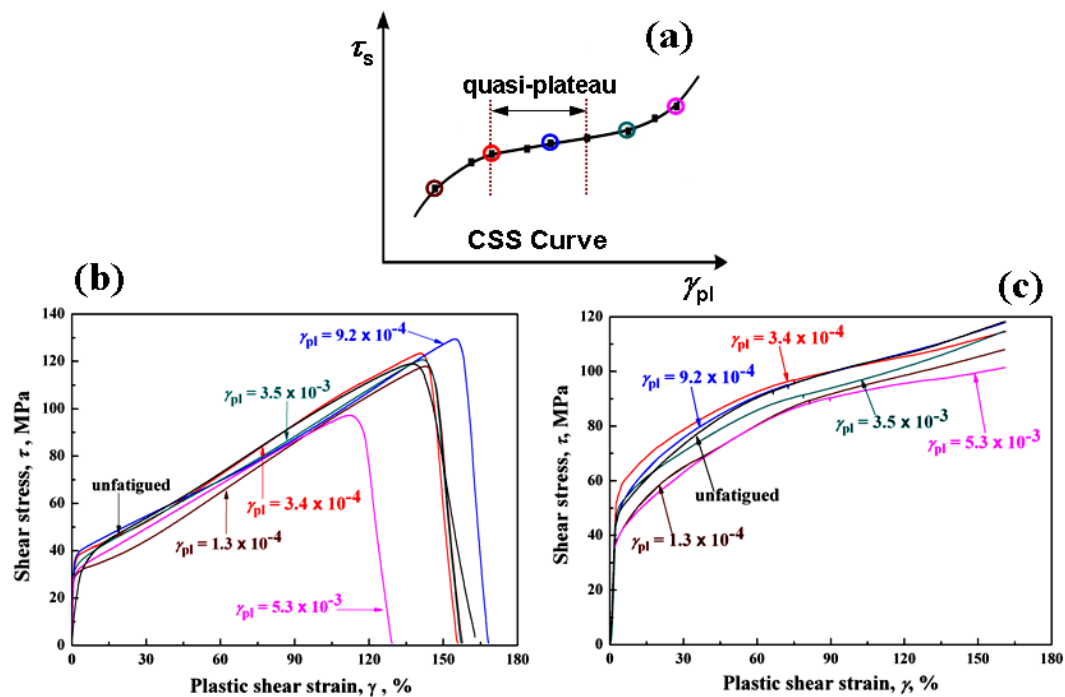


Figure 1. (a) CSS curve of $[\bar{2}33]$ Cu single crystals [10]; (b) the tensile and (c) compressive stress-strain curves of $[\bar{2}33]$ Cu single crystals unfatigued and pre-fatigued at different plastic strain amplitudes.

From Figure 1b it can be seen that, compared to the unfatigued specimen, the yield strength slightly increases but the tensile strength and elongation basically remain unchanged for the specimens pre-fatigued at two low γ_{pl} of 1.3×10^{-4} and 3.4×10^{-4} , which are located below the quasi-plateau region in the CSS curve (Figure 1a). As the pre-fatigue strain amplitude, e.g., 9.2×10^{-4} , is exactly located in the quasi-plateau region in the CSS curve, both strength and elongation are coincidentally improved. As γ_{pl} increases to 3.5×10^{-3} , which is beyond the quasi-plateau region in the CSS curve, the yield and tensile strengths and elongation become comparable to those of the unfatigued specimen. With further increasing γ_{pl} to 5.3×10^{-3} , both strength and elongation decrease obviously, and even become much lower than those of the unfatigued specimen. Accordingly, only when the crystal is pre-fatigued at an intermediate γ_{pl} of 9.2×10^{-4} , the strengthening effect due to low-cycle fatigue training is the most notable.

From Figure 1c one can see that the general rule for the effect of pre-cycling on the compressive mechanical properties (e.g., compressive yield strength and flow stress) is basically similar to the tensile case (Figure 1b); however, the difference in the compressive properties of the specimens pre-cycled at different γ_{pl} is not so noticeable as compared to the difference in tensile properties.

3.2. Deformation Features on the Surface

Figures 2 and 3 present the essential surface deformation features of the unfatigued and pre-fatigued $[\bar{2}33]$ Cu single-crystal specimens under tensile and compressive deformation, respectively.

Only a few slip bands appear in some regions and distribute inhomogeneously on the specimen surface after pre-cycling at $\gamma_{pl} \leq 3.4 \times 10^{-4}$ [10], indicating that strain hardening induced by pre-cycling is not significant in this case, so that the tensile properties of the specimens pre-fatigued at these low γ_{pl} are nearly not improved as compared to those of the unfatigued specimen (Figure 1b). Correspondingly, the tensile deformation features indicated by Figure 1a–c are almost similar. It should be mentioned that $[\bar{2}33]$ is a coplanar-slip orientation, i.e., the primary and secondary slip planes are the same plane (111); thus only single-oriented slip bands can be generally observed on the surface under pre-fatigue and tensile deformation (Figure 2a–c).

As γ_{pl} increases to 9.2×10^{-4} , a few deformation concentration regions, i.e., deformation bands (DBs), are formed, and the formation of such preliminary DBs may cause a notable cyclic hardening but does not bring about an obvious damage [10], and therefore, the working hardening capacity during subsequent tension is enhanced, as evidenced by the co-operation of the conjugate slip system $(\bar{1}11)[011]$ under tensile deformation (Figure 3d). Therefore, the tensile strength has been improved. It should be mentioned here that it is unnecessary for the operation of the conjugate slip system to accommodate plastic strain during pre-fatigue deformation [10]. Furthermore, the inducement of such preliminary DBs by pre-cycling should be beneficial to the subsequent tensile plastic deformation along these concentrated bands, so the tensile ductility (or elongation) is also somewhat increased (Figure 1b).

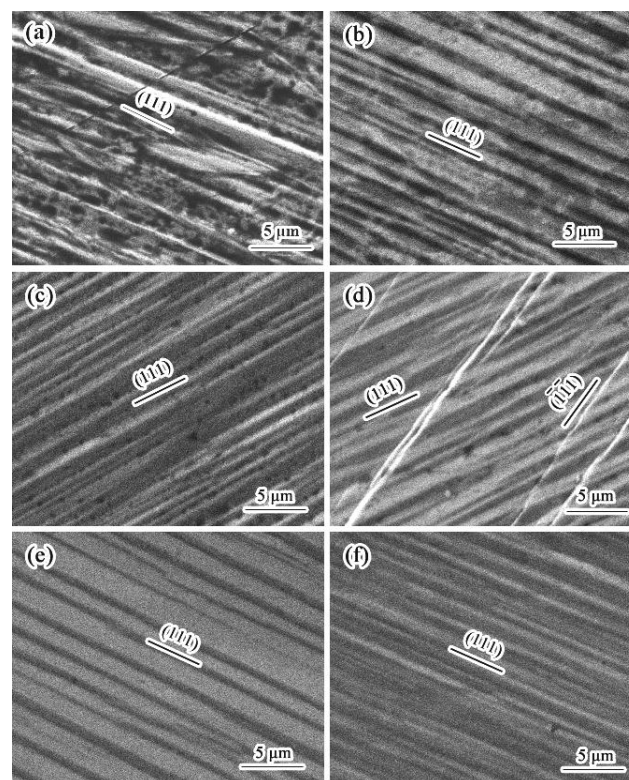


Figure 2. SEM images of the surface deformation features of unfatigued or pre-fatigued $[\bar{2}33]$ Cu single crystals under uniaxial tension: (a) unfatigued; (b–f) pre-fatigued at $\gamma_{pl} = 1.3 \times 10^{-4}$, 3.4×10^{-4} , 9.2×10^{-4} , 3.5×10^{-3} , and 5.3×10^{-3} , respectively. (a,b,e,f) viewed from $(\bar{6} \ 9 \ \bar{1}3)$; and (c,d) viewed from $(6 \ \bar{9} \ 13)$. Note that the loading direction is horizontal.

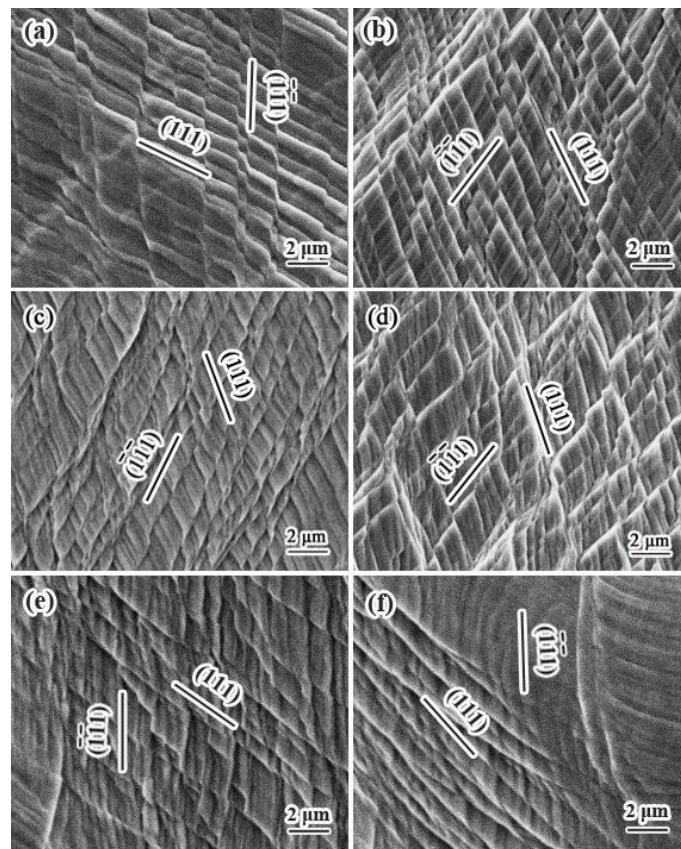


Figure 3. SEM images of the surface deformation features of unfatigued or pre-fatigued $[2\bar{3}3]$ Cu single crystals under uniaxial compression: (a) unfatigued, (b–f) pre-fatigued at $\gamma_{pl} = 1.3 \times 10^{-4}$, 3.4×10^{-4} , 9.2×10^{-4} , 3.5×10^{-3} , and 5.3×10^{-3} , respectively. (a,e,f) viewed from $(\bar{6} \ 9 \ \bar{1}3)$; and (b–d) viewed from (320) . Note that the loading direction is horizontal.

However, at high strain amplitudes ($\gamma_{pl} \geq 3.5 \times 10^{-3}$), many highly concentrated DBs are formed and severe fatigue damage has been introduced [10], so that the subsequent tensile properties cannot be effectively enhanced. In particular, when γ_{pl} is as high as 5.3×10^{-3} , the induced permanent damage in the form of densely distributed DBs becomes extremely notable [10], thus causing a greatly detrimental effect on the subsequent tensile properties, i.e., the strength and ductility decrease obviously to much lower values than those of other specimens. Correspondingly, the density of slip bands is relatively low and, also, the conjugate slip system $(\bar{1}\bar{1}1)[011]$ is not activated (Figure 2e,f) after the tensile deformation of those specimens pre-fatigued at high γ_{pl} .

Compared to the case of tensile deformation, the stress state under compressive deformation is much more beneficial to the continuation of plastic flow deformation. Therefore, the secondary (conjugate) slip system $(\bar{1}\bar{1}1)[011]$ is commonly activated under compression (Figure 3). Furthermore, the subsequent compressive deformation behavior is not so sensitive to the damage induced by pre-cycling, so that the deformation features are basically similar for all the specimens unfatigued or pre-fatigued at different γ_{pl} , as shown in Figure 3, and no marked difference in the relevant compressive stress-strain curves is manifested (Figure 1c).

3.3. Dislocation Structures

Figure 4 shows the tensile dislocation structures of $[2\bar{3}3]$ Cu single crystals unfatigued or pre-fatigued at different γ_{pl} , where \mathbf{g} is the diffraction vector and \mathbf{B} is the incident beam. It is found that the dislocation structures of those specimens unfatigued or pre-fatigued at low γ_{pl} of 1.3×10^{-4} and 3.4×10^{-4} are typically featured by dislocation cells (Figure 4a–c); however, for

pre-fatigued specimens, the cell walls are relatively loose and the average cell diameter is $\sim 0.5 \mu\text{m}$ (as representatively shown in Figure 4b,c), indicating that the plastic strain accommodated during the tensile process of specimens pre-fatigued at low γ_{pl} is not so high, and their strain-hardening abilities are thus basically equivalent to that of the unfatigued specimen (Figure 1b). As the pre-fatigue strain amplitude γ_{pl} increases to 9.2×10^{-4} , the dislocation density of the cell walls becomes obviously increased, and the cell diameter reduces to $\sim 0.3 \mu\text{m}$ (Figure 4d), showing a stronger strain-hardening ability of the specimen pre-fatigued at such a γ_{pl} (Figure 1b). As γ_{pl} further increases to higher values of 3.5×10^{-3} or 5.3×10^{-3} , the dislocation cells become loose again, and the average cell diameter is increased to $0.6\text{--}0.7 \mu\text{m}$ (Figure 4e,f). Our previous work [11,12] has revealed that the fatigue dislocation structures of $[\bar{2}33]$ Cu single crystals were mainly composed of dislocation cells, the size of which decreased with increasing γ_{pl} . Moreover, as $\gamma_{\text{pl}} \geq 3.5 \times 10^{-3}$, the configuration of fatigue-induced dislocation cells exhibited a characteristic of a persistent slip band (PSB) ladder-like structure, and these dislocation cells were thus called PSB cells, showing a severe strain concentration and deformation damage [11,12]. In this way, during the subsequent tensile deformation, the serious strain concentration will easily occur at these PSB cells, thus leading to an earlier fracture failure at a lower tensile flow stress and strain levels (Figure 1b). In general, as shown in Figures 1b and 4, the strength values increase with the decreasing cell diameter; this phenomenon is consistent with the general relation of saturation stress vs. dislocation cell size for fatigued Cu single crystals [13].

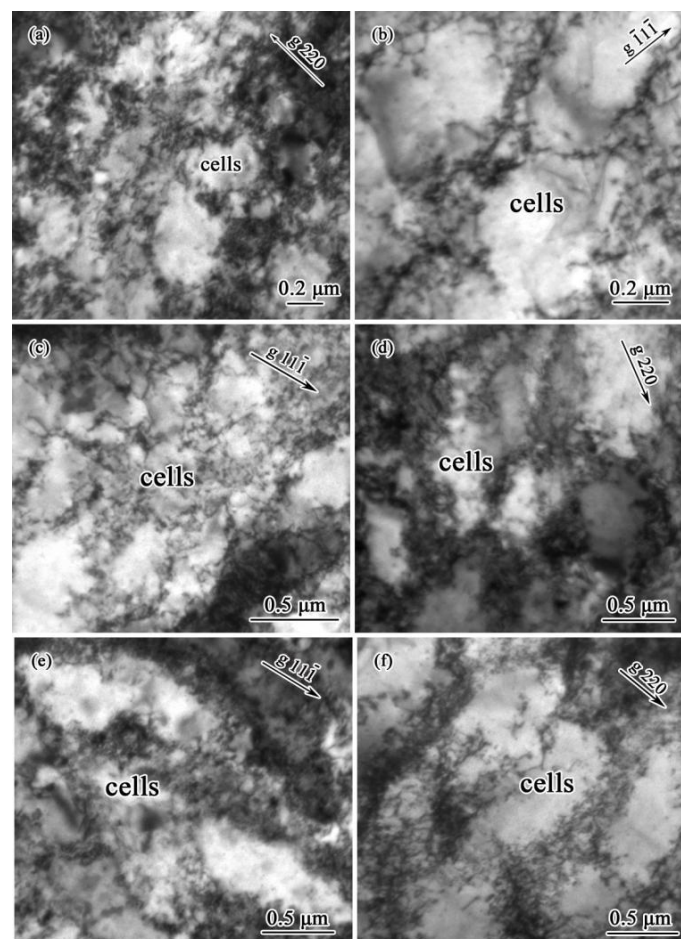


Figure 4. TEM images of dislocation configurations of unfatigued or pre-fatigued $[\bar{2}33]$ Cu single crystals under uniaxial tension: (a) unfatigued, $\mathbf{B} = \bar{1}13$; pre-fatigued at (b) $\gamma_{\text{pl}} = 1.3 \times 10^{-4}$, $\mathbf{B} = \bar{1}12$; (c) $\gamma_{\text{pl}} = 3.4 \times 10^{-4}$, $\mathbf{B} = 011$; (d) $\gamma_{\text{pl}} = 9.2 \times 10^{-4}$, $\mathbf{B} = \bar{1}11$; (e) $\gamma_{\text{pl}} = 3.5 \times 10^{-3}$, $\mathbf{B} = 011$; and (f) $\gamma_{\text{pl}} = 5.3 \times 10^{-3}$, $\mathbf{B} = \bar{1}11$.

Figure 5 shows the compressive dislocation structures of $[\bar{2}33]$ Cu single crystals unfatigued or pre-fatigued at different γ_{pl} . The dislocation structure of the unfatigued specimen consists of equiaxed dislocation cells (Figure 5a). For the pre-fatigued specimen at $\gamma_{pl} = 1.3 \times 10^{-4}$, the dislocation cells become very loose (Figure 5b), and the relevant compressive flow stress is low (Figure 1c). As γ_{pl} increases to 3.4×10^{-4} and 9.2×10^{-4} , the dislocation density of cell walls increases greatly, and the compressive plastic flow undergoes relatively high stress levels (Figure 1c). It means that the strain-hardening ability can be somewhat improved after the $[\bar{2}33]$ Cu single crystal was pre-fatigued at these two γ_{pl} , although such an improvement is not as obvious as the case of tensile deformation. As γ_{pl} increases to 3.5×10^{-3} , the dislocation structure is featured by some loose dislocation cells (Figure 5e), corresponding to a decreased compressive flow stress (Figure 1c). As $\gamma_{pl} = 5.3 \times 10^{-3}$, the compressive dislocation structure becomes regularly arranged equiaxed dislocation cells (Figure 5f); however, the compressive flow stress level is not high, but at the lowest level (Figure 1c). Therefore, it is inferred that some of the equiaxed dislocation cells induced by pre-fatigue deformation [12] may be retained in the crystal subjected to subsequent compressive deformation, as shown in Figure 5f.

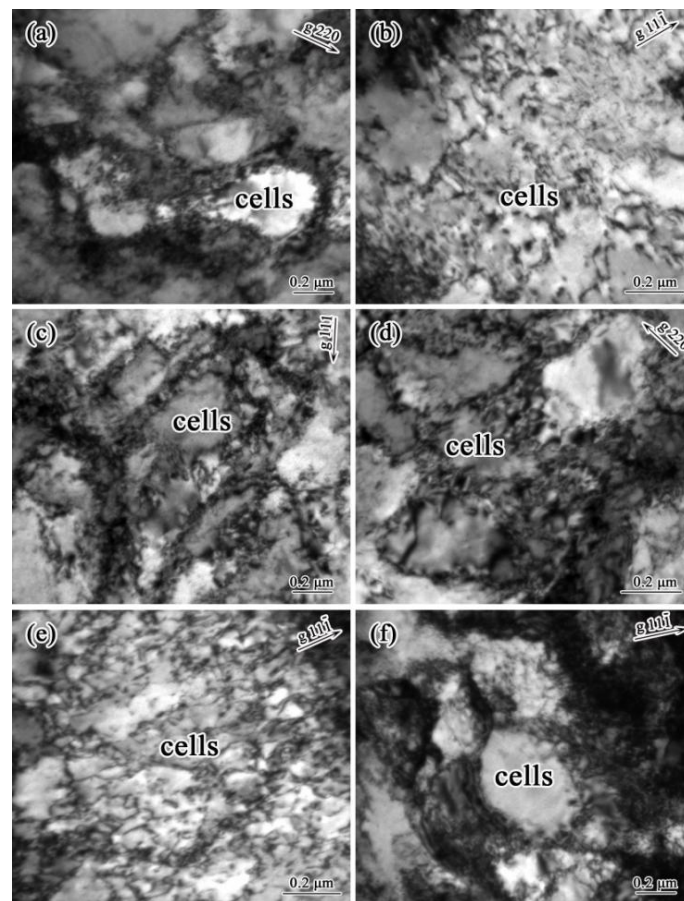


Figure 5. TEM images of dislocation configurations of unfatigued or pre-fatigued $[\bar{2}33]$ Cu single crystals under uniaxial compression: (a) unfatigued, $\mathbf{B} = \bar{1}11$; pre-fatigued at (b) $\gamma_{pl} = 1.3 \times 10^{-4}$, $\mathbf{B} = 011$; (c) $\gamma_{pl} = 3.4 \times 10^{-4}$, $\mathbf{B} = \bar{1}01$; (d) $\gamma_{pl} = 9.2 \times 10^{-4}$, $\mathbf{B} = \bar{1}11$; (e) $\gamma_{pl} = 3.5 \times 10^{-3}$, $\mathbf{B} = 011$; and (f) $\gamma_{pl} = 5.3 \times 10^{-3}$, $\mathbf{B} = 011$.

As is well known, the equal-channel angular pressing (ECAP) technique has recently become one of the most frequently used mechanical processing methods to produce ultrafine-grained (UFG) materials by introducing intensive plastic strain into materials after repetitive pressing [14,15]. It should be mentioned that the term “ultrafine-grained”, widely used by the ECAP community, sometimes (e.g., UFG pure Cu) represents a microstructure comprising very fine, highly misoriented

dislocation cells or subgrains [16–19]. Such ultrafine-celled (the cell diameter is around some hundred nanometers) microstructures produced by the ECAP severe plastic deformation technique normally exhibit an extraordinarily high strength but are followed by a great loss of ductility, although a subsequent, controlled short-term annealing treatment might cause a joint enhancement of strength and ductility [20]. In contrast, the cell structure developed under fatigue deformation is well recognized to be a typical type of heterogeneous dislocation distribution, and high-symmetry orientations, low friction stress, large deformation and the easy operation of cross slip favor the formation of dislocation cell structures [21]. For the present $[\bar{2}33]$ orientation, dislocation reactions between the primary and coplanar slip systems produce the third Burgers vector contained in the same (111) plane, i.e., $(a/2)[\bar{1}01] + (a/2)[1\bar{1}0] \rightarrow (a/2)[0\bar{1}1]$. The produced dislocation $(a/2)[0\bar{1}1]$ is also glissile in the common primary slip plane (111). Such a dislocation reaction would promote the much easier formation of slightly misoriented dislocation cells during fatigue deformation [11,22], and the cell diameter is also around some hundred nanometers depending upon the applied strain amplitude [11,12]. Apparently, the dislocation cell structures directly produced by fatigue cycling are more uniformly distributed and the dislocation density is relatively lower compared with UFG microstructures. Accordingly, under the prerequisite that no obvious pre-damage is introduced, the inducement of such a uniformly distributed low-dislocation-density cell structure through an appropriate pre-fatigue deformation treatment may, more or less, improve the static strength and ductility together, e.g., pre-fatigue at $\gamma_{pl} = 9.2 \times 10^{-4}$ in the present work. This phenomenon is normally called strengthening by low-cycle fatigue (LCF) training.

4. Conclusions

The effect of pre-fatigue deformation at different plastic strain amplitudes on the monotonic tensile and compressive deformation behavior of the $[\bar{2}33]$ coplanar double-slip-oriented Cu single crystal was experimentally investigated. The following conclusions can be drawn:

- (1) As the $[\bar{2}33]$ crystal specimen is pre-fatigued at a plastic strain amplitude γ_{pl} of 9.2×10^{-4} , which is located within the quasi-plateau of the CSS curve, its tensile strength and ductility can be coincidentally improved, showing an obvious strengthening effect by LCF training, since uniformly distributed dislocation cell structures have been reasonably introduced by pre-fatigue cycling. In contrast, for the crystal specimens pre-fatigued at γ_{pl} lower or higher than the quasi-plateau region, due to a low pre-cyclic hardening or pre-induction of fatigue damage, there is no marked strengthening effect by LCF training, and a weakening effect by LCF damage occurs.
- (2) The general rule for the effect of pre-fatigue deformation on the uniaxial compressive behavior follows a similar pattern as the case of uniaxial tension, but such an effect is not so significant, since the stress state under compressive deformation is much more beneficial to the continuation of plastic flow deformation and the compressive deformation behavior is insensitive to damage induced by pre-cycling.

Acknowledgments: This work was financially supported by the National Natural Science Foundation of China (NSFC) under Grant Nos. 51271054, 51231002 and 51571058.

Author Contributions: X.-W.L. designed the scope of the paper. X.-M.W., W.-W.G. and C.-J.Q. participated in the sample preparation and all experiments. X.-W.L., Y.Y. and X.-M.W. analyzed the experimental results. X.-W.L. wrote this paper.

Conflicts of Interest: The authors declare no conflict of interest.

References

1. Santana, U.S.; Gonzalez, C.R.; Mesmacque, G.; Amrouche, A.; Decoopman, X. Dynamic tensile behavior of materials with previous fatigue damage. *Mater. Sci. Eng. A* **2008**, *497*, 51–60. [[CrossRef](#)]
2. Santana, U.S.; Gonzalez, C.R.; Mesmacque, G.; Amrouche, A. Effect of fatigue damage on the dynamic tensile behavior of 6061-T6 aluminum alloy and AISI 4140T steel. *Int. J. Fatigue* **2009**, *31*, 1928–1937. [[CrossRef](#)]

3. Ye, D.Y.; Xu, Y.D.; Xiao, L.; Cha, H.B. Effects of low-cycle fatigue on static mechanical properties, microstructures and fracture behavior of 304 stainless steel. *Mater. Sci. Eng. A* **2010**, *527*, 4092–4102. [[CrossRef](#)]
4. Yan, Y.; Lu, M.; Li, X.W. Effects of pre-fatigue deformation on the uniaxial tensile behavior of coarse-grained pure Al. *Acta Metall. Sin.* **2013**, *49*, 658–666. (In Chinese) [[CrossRef](#)]
5. Yan, Y.; Lu, M.; Guo, W.W.; Li, X.W. Effect of pre-fatigue deformation on the thickness-dependent tensile behavior of coarse-grained pure aluminum sheets. *Mater. Sci. Eng. A* **2014**, *600*, 99–107. [[CrossRef](#)]
6. Li, X.W.; Wang, X.M.; Guo, W.W.; Qi, C.J.; Yan, Y. Effect of cyclic pre-deformation on the uniaxial tensile deformation behavior of [017] copper single crystals oriented for critical double slip. *Metall. Mater. Trans. A* **2013**, *44*, 1631–1635. [[CrossRef](#)]
7. Li, X.W.; Zhang, Z.F.; Wang, Z.G.; Li, S.X.; Umakoshi, Y. SEM-ECC Investigation of dislocation arrangements in cyclically deformed copper single crystals with different crystallographic orientations. *Defect Diffus. Forum* **2001**, *188–190*, 153–170. [[CrossRef](#)]
8. Li, X.W.; Umakoshi, Y.; Gong, B.; Li, S.X.; Wang, Z.G. Dislocation structure in fatigued critical and conjugate double-slip-oriented copper single crystals. *Mater. Sci. Eng. A* **2002**, *333*, 51–59. [[CrossRef](#)]
9. Li, X.W. Monotonic and cyclic deformation in single crystal [A]. In *The Encyclopedia of Tribology*; Wang, Q.J., Chung, Y.-W., Eds.; Springer Science+Business Media: New York, NY, USA, 2013; Chapter 248; Volume 260, pp. 2313–2323.
10. Li, X.W.; Wang, Z.G.; Li, S.X. Cyclic deformation behavior of double-slip-oriented copper single crystals I. Coplanar double slip orientation on 011-111 side in the stereographic triangle. *Mater. Sci. Eng. A* **1999**, *260*, 132–138. [[CrossRef](#)]
11. Li, X.W.; Wang, Z.G.; Zhang, Y.W.; Li, S.X.; Umakoshi, Y. Dislocation structure in cyclically deformed coplanar double-slip-oriented copper single crystals. *Phys. Status Solidi* **2002**, *191*, 97–105. [[CrossRef](#)]
12. Zhou, Y.; Li, X.W.; Yang, Q.R. Study of Fatigue dislocation structures in $\bar{2}33$ coplanar double-slip-oriented copper single crystals using SEM electronic channelling contrast. *Int. J. Mater. Res.* **2008**, *99*, 958–963. [[CrossRef](#)]
13. Suresh, S. *Fatigue of Materials*, 2nd ed.; Cambridge University Press: London, UK, 1998.
14. Valiev, R.Z.; Islamgaliev, R.K.; Alexandrov, I.V. Bulk nanostructured materials from severe plastic deformation. *Prog. Mater. Sci.* **2000**, *45*, 103–189. [[CrossRef](#)]
15. Valiev, R.Z. Materials science: Nanomaterial advantage. *Nature* **2002**, *419*, 887–889. [[CrossRef](#)] [[PubMed](#)]
16. Agnew, S.R.; Weertman, J.R. Cyclic softening of ultrafine grain copper. *Mater. Sci. Eng. A* **1998**, *244*, 145–153. [[CrossRef](#)]
17. Torre, F.D.; Lapovok, R.; Sandlin, J.; Thomson, P.F.; Davies, C.H.J.; Pereloma, E.V. Microstructures and properties of copper processed by equal channel angular extrusion for 1–16 passes. *Acta Mater.* **2004**, *52*, 4819–4832. [[CrossRef](#)]
18. Kong, M.K.; Kao, W.P.; Lui, J.T.; Chang, C.P.; Kao, P.W. Cyclic deformation of ultrafine-grained aluminium. *Acta Mater.* **2007**, *55*, 715–725.
19. Jiang, Q.W.; Li, X.W. Effect of pre-annealing treatment on the compressive deformation and damage behavior of ultrafine-grained copper. *Mater. Sci. Eng. A* **2012**, *546*, 59–67. [[CrossRef](#)]
20. Mughrabi, H.; Höppel, H.W.; Kautz, M.; Valiev, R.Z. Annealing treatments to enhance thermal and mechanical stability of ultrafine-grained metals produced by severe plastic deformation. *Z. Met.* **2003**, *94*, 1079–1083. [[CrossRef](#)]
21. Mughrabi, H. Dislocation wall and cell structures and long-range internal stresses in deformed metal crystals. *Acta Metall.* **1983**, *31*, 1367–1379. [[CrossRef](#)]
22. Jin, N.Y.; Winter, A.T. Cyclic deformation of copper single crystals oriented for double slip. *Acta Metall.* **1984**, *32*, 989–995. [[CrossRef](#)]

